Terr. Atmos. Ocean. Sci., Vol. 32, No. 6, Part III, 1289-1302, December 2021 doi: 10.3319/TAO.2021.12.30.04

Post-collisional and volcanic features of the Late Miocene-Pleistocene foreland area, northern offshore Taiwan

Ho-Han Hsu[1, 2], Eason Yi-Cheng Yang[3], Jih-Hsin Chang[1, *], Chih-Chieh Su[1], Char-Shine Liu[2], Shye-Donq Chiu[1], and Jen-Sen Shen[4]

[1] *Institute of Oceanography, National Taiwan University, Taipei City, Taiwan*
[2] *Ocean Center, National Taiwan University, Taipei City, Taiwan*
[3] *Exploration and Production Business Division, CPC, Taipei City, Taiwan*
[4] *Bureau of Mines, Ministry of Economic Affairs, Taipei City, Taiwan*

Article history:
Received 27 September 2021
Revised 13 December 2021
Accepted 30 December 2021

Keywords:
Wedge-top, Post collision, Volcanism, Taiwan

Citation:
Hsu, H.-H., E. Y.-C. Yang, J.-H. Chang, C.-C. Su, C.-S. Liu, S.-D. Chiu, and J.-S. Shen, 2021: Post-collisional and volcanic features of the Late Miocene-Pleistocene foreland area, northern offshore Taiwan. Terr. Atmos. Ocean. Sci., 32, 1289-1302, doi: 10.3319/TAO.2021.12.30.04

ABSTRACT

Based on multichannel seismic data northern offshore Taiwan, we revisited the post-collisional and volcanic features in the Late Miocene-Pleistocene wedge-top of the early Taiwan orogenic wedge. Seismic data transverse to wedge-top zone show the asymmetric and symmetric folds, along with blind thrusts and back thrusts. Seismic data parallel to the axis of the wedge-top zone show the volcanic features of poor stratified reflectors, forced fold and intrusive step of volcanic sills along and away from dominating normal fault structures. Since the volcanic extrusions and normal faults are probably associated events, we suggest that post-collisional extensional volcanism northern offshore Taiwan was probably formed along inherited primary and secondary fault structures. The wedge-top zone was formed at frontal part of the early Taiwan orogenic wedge in Late Miocene. Subsequent change of regional stress from convergence to extension led to the mountain collapse as well as primary and secondary normal faults. Thus, these post-collisional normal faults are mechanically weak, probably capable of providing pathways for the Pleistocene-present volcanisms northern offshore Taiwan. The facilitation of post-collisional fault structures as transportation routes for deep material to migrate along may be important for the formation of the Quaternary volcanism extrusions northern offshore Taiwan.

1. INTRODUCTION

In a convergent setting, the transition from collision to post-collision may result in change of structural styles and magmatic activities (Williams et al. 2001; Chung et al. 2005; Jolivet and Brun 2010; Seghedi et al. 2011; Pace et al. 2017). When the regional stress changes from convergence to extension, the convergent collisional mountain belt will start to collapse and subside once the sense of faulting has changed from reverse to normal. The post-collision magmatism, one of the common features of many orogens, will occur and produce magma associated with extensional processes. The regional extension of the post-collision is major driver of these changes of structural styles and magmatic activities, while the relationship between the post-collisional volcanisms and structures receives few attentions.

Taiwan is formed by oblique collision between Luzon Arc and Eurasian continent since Late Miocene (Fig. 1a; Teng 1990). As Taiwan orogenic wedge grew dischronously from north to south and climax occurs at central Taiwan, northern Taiwan is now in its post-collision state (Teng 1996; Liu et al. 2001). Taipei Basin in northern Taiwan, for example, is a Quaternary extensional basin and considered as a post-collision basin (Fig. 1b, Teng et al. 2001). The Quaternary structures in northern offshore Taiwan are dominated by re-activated extensional normal faults, suggesting currently a post-collision state (Hsiao et al. 1998). On the other hand, Quaternary volcanisms in northern Taiwan are commonly found on frontal part of the Late Miocene-Pleistocene orogenic wedge (hereafter wedge-top, Fig. 1c) and has provided good constraints on post-collision state as well (Fig. 2; Wang et al. 1999, 2002, 2004; Chung et al. 2001). However, it seems that integration of volcanisms

* *Corresponding author*
E-mail: changjihhsin@ntu.edu.tw

and structural development into evolutionary history of northern Taiwan have not been fully considered and requires more discussion.

The objective of this study is to provide more observations of fault structures and volcanism northern offshore Taiwan, and to investigate their possible relationship with multichannel seismic (MCS) data, a powerful tool to explore the geometry and connectivity of magma conduit controlled by interactions between tectonic and magmatic process. With the Quaternary post-collision structures and volcanisms, northern offshore Taiwan provides an excellent place to discuss the possible relationship between post-collision volcanisms and structures. In this study, we firstly revisited the fault structures that probably have influence on the Quaternary volcanism northern offshore Taiwan, based on our MCS data. Then, we discussed the distribution of volcanic intrusions and extrusions based on published results and our observations in this study. After determination of the possible relationship between fault structures and volcanism, we updated the current regional evolution model of northern and offshore Taiwan with an integration of the fault structure and volcanism. The result may widen current understanding of the regional volcanisms northern offshore Taiwan within the structural evolutional framework.

Although the seismic imaging directly beneath sills may be commonly poor because of attenuation of acoustic energy within igneous rocks, sill complexes are relatively well imaged in seismic data because igneous commonly have greater densities and seismic velocity compared to the surrounding sediment strata (Magee et al. 2016). Sill emplaced in strata are shown in variable morphology like intrusive steps, broken bridges, and magma fingers (Fig. 3;

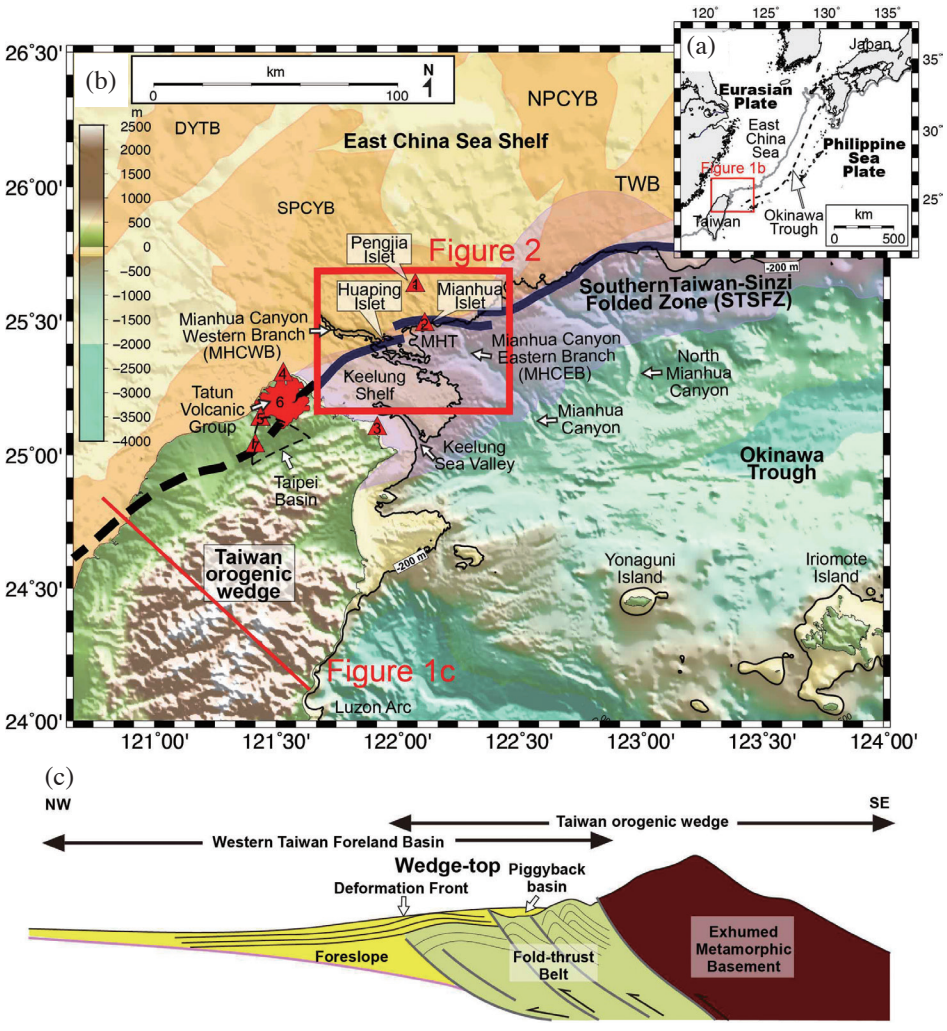

Fig. 1. Geographic and geological context of the study area. (a) map showing study area in East Asia. (b) Map showing study area, covering the East China Sea Shelf, Southern Taiwan-Sinzi Folded Zone (purple area), Okinawa Trough and Taiwan orogenic wedge. Orange areas indicate the distribution of pre-Miocene basin, including Dongyintao Basin (DYTB), Northern Pengchiayu Basin (NPCYB), Southern Pengchiayu Basin (SPCYB), and Taiwan Basin (TWB). Thin black lines indicate the -200 m isobaths, representing the approximate location of shelfbreak. (c) Schematic geological profile of the Taiwan orogenic wedge. The wedge-top zone is part of the foreland basin system that most close to hinterland (modified from Chang et al. 2012).

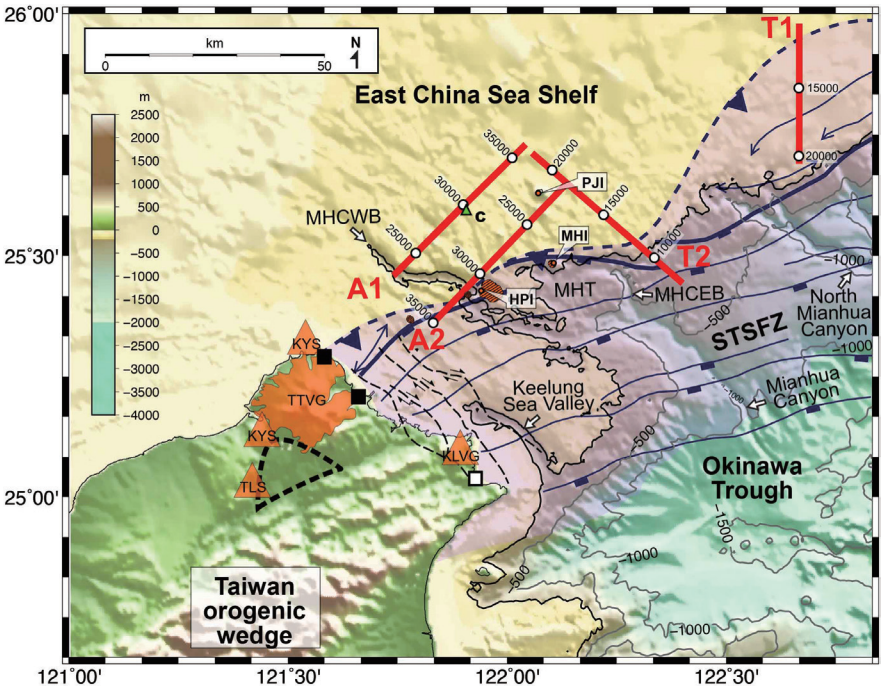

Fig. 2. Data distribution and structural framework of the South Taiwan-Sinzi Folded Zone northern offshore Taiwan. Red lines indicate MCS survey lines, denoted as T1 (Fig. 4), T2 (Fig. 5), A1 (Fig. 6), and A2 (Fig. 7). The values nearby white circles on the red lines indicate shot point number. Barbed line indicates the deformation front (Hsiao et al. 1998). Orange circles, triangles and areas indicate the Northern Taiwan Volcanic Zone (PJI: PengJia Islet; MHI: Mianhua Islet; HPI: Huaping Islet; KLVG: Keelung Volcanic Group; KYS: Kuanyinshan; TTVG: Tatun Volcanic Group; TLS: Tsaolinshan). The empty triangle indicates the drilling site. The filled and empty squares indicate the operating and underconstructed nuclear power plants, respectively. Locations of the normal faults in STSFZ and offshore volcanic bodies are referred to Hsiao et al. (1998).

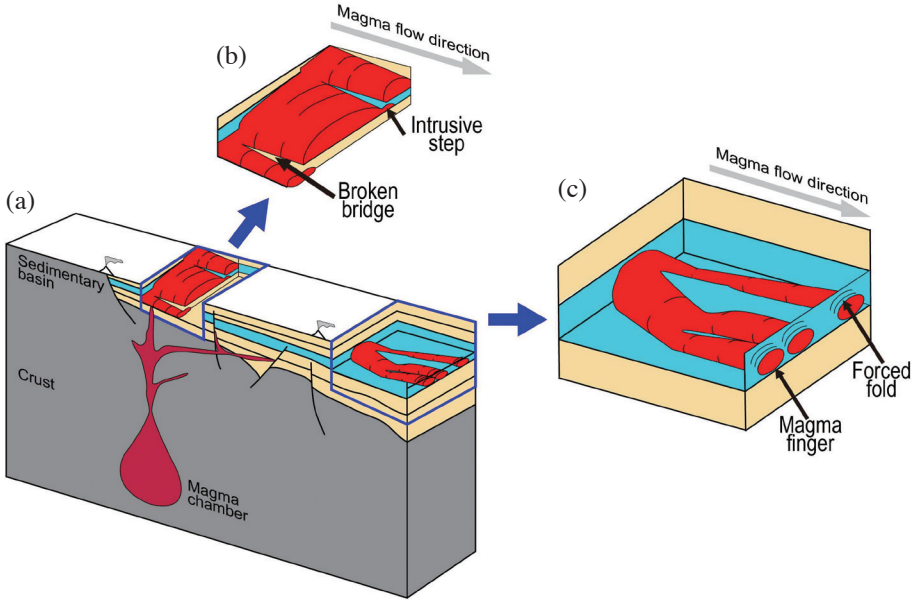

Fig. 3. Schematic diagrams showing the ascending magma from deep crust to sedimentary basin and emplacement of sill complex. (a) Crustal scale diagram showing magma ascend from magma chamber to a sedimentary basin. (b) Schematic diagram showing interlayer migration of magma. Broken bridge forms when two separate overlapping magmatic sheet segments propagate contemporaneously along slightly offset horizons. Intrusive steps forms when magma migrates between different layers. (C) Schematic diagram showing the tube-like structures of magma fingers (modified from Magee et al. 2016).

Pollard et al. 1975; Schofield et al. 2010, 2012; Magee et al. 2016; Spacapan et al. 2017). These features are commonly served as magma flow indicators and may be largely controlled by host rock lithology.

The sill complex may develop along the strata, as long as the inherited structures. In offshore Norway, layer parallel reflectors and saucer-shaped reflectors are recognized, showing the smoothness, size, continuity and depth of paleosurfaces of the sill (Planke et al. 2005). It is commonly seen that a forced fold will be formed when sills are emplaced at shallow levels (Jackson et al. 2013; Reeves et al. 2018). Besides, the location and geometry of basaltic intrusion bodies are strongly controlled by pre-existing structures and local stress (Valentine and Krogh 2006). Pre-existing fractures are likely to be reactivated as magma conduits where deformed hanging wall fault plane corrugation alter the orientation of the principal stress axes (Magee et al. 2013). Pre-existing structures, therefore, may play an important role in magma ascending and the formation of volcanic extrusions and intrusions subsurface.

2. TECTONIC BACKGROUND

The tectonics and structures north offshore Taiwan feature the collapsed Late Miocene-Pleistocene wedge-top zone of the early Taiwan orogenic wedge (Fig. 1c). In north offshore Taiwan, the Late Miocene-Pleistocene wedge-top zone has diminished and collapsed because of the southward migration of the Taiwan orogenic wedge. The area of the collapsed Late Miocene-Pleistocene wedge-top zone is currently submerged and is dominated by post-collisional faults and volcanic structures (Hsiao et al. 1998; Wang et al. 2004). The features of the collapsed Late Miocene-Pleistocene wedge-top zone can be observed in terms of the bathymetry, structures, and magmatism.

2.1 Bathymetry

Northern offshore Taiwan is dominated by shelf and shelf-slope environment, including East China Sea Shelf, Keelung Shelf, Keelung Sea Valley, Mianhua Canyon and North Mianhua Canyon (Figs. 1 and 2; Song et al. 2000; Yu and Song 2000). The Keelung Shelf, bounded between Mianhua Canyon and Keelung Sea Valley, is morphologically distinguished from East China Sea Shelf by a rugged seafloor of tens of meters of relief. Also, there are several linear fault scarps found in Keelung Shelf. It is thus suggested that the Keelung Shelf is a tectonic-dominated environment (Song et al. 1997).

The sea valley and submarine canyons are oriented roughly NW-SE and cut the shelf area, forming trough-shaped and indented channels. Among these submarine valley and canyons, Keelung Sea Valley runs parallel to the coastline off northern Taiwan and defines the Keelung Shelf to the north. The western branch of the Mianhua Canyon (Hereafter MHCWB; Chang et al. 2021) around the Mianhua Islet and Huaping Islet indented about 120 km into the shelfbreak, showing a great distance of indention far beyond other canyons and could be considered as the most striking bathymetry feature on the shelf area (Figs. 1 and 2; Song et al. 2000).

2.2 Late Miocene-Pleistocene Wedge Top Zone

Before Taiwan orogenic wedge was formed, it was part of the northernmost passive margin of the South China Sea with well-developed shelf-slope-rise settings (Teng 1992; Yu and Chou 2001). Several rifting basins are present in northern offshore Taiwan: at inner shelf, the Tungyintao, which is bounded by rifting faults, at outer shelf the Taiwan, North and South Pengchiayu Basins are contemporaneous rifting basins covered by Neogene sedimentary sequence (Fig. 1b; Teng 1992; Chen and Watkins 1994).

Since Late Miocene, Taiwan orogenic wedge was formed by oblique collision between Luzon arc and Eurasian continent, growing dischronously from north to south and climax occurs at central Taiwan (Teng 1990, 1996; Liu et al. 2001). The earliest Taiwan orogenic wedge was formed northern offshore current Taiwan, known as Southern Taiwan-Sinzi Folded Zone (STSFZ; Figs. 1 and 2; Hsiao et al. 1998; Kong et al. 2000). After Taiwan orogeny migrated southward, the regional stress was changed from compressive to extensional (Teng 1996; Hsiao et al. 1998). Accordingly, the tectonic domain of northern Taiwan was changed from collisional orogenic wedge to post-collisional collapsing mountain ranges.

A wedge-top zone occurs along the cratonward part of the orogenic wedge and includes piggyback basins on the top of (buried) structural fold-thrust belt, indicating a tectono-sedimentary domain (Fig. 1c; DeCelles and Giles 1996; Chiang et al. 2004; DeCelles 2011). As a cratonward part of the Taiwan orogeic wedge, the collapsed Late Miocene-Pleistocene wedge-top zone of the Taiwan orogenic wedge is now located on the shelf, approximately along the western boundary of the STSFZ. It is also the region where most post-collisional volcanisms occurred in northern offshore Taiwan.

2.3 Regional Structures

The structures northern offshore Taiwan are dominated by NE-SW faults (Huang et al. 1992; Chen and Watkins 1994; Hsiao et al. 1994, 1998) and NW-SE lineaments (Song et al. 2000). The NE-SW faults were formed by a series of regional Palaogene rifting extension (Yu and Chow 1997), Late Miocene reactivate thrusting, and Late Pliocene reactivating normal faulting, reflecting transitions of tectonic environments from passive margin, to fold-thrust belt,

and mountain collapse. The NW-SE lineaments may result from strike-slip movement in response to indenting Taiwan orogenic wedge (Song et al. 2000).

The northern offshore Taiwan is currently in an extension state (Teng 1996) and is predominated by a set of NE-SW normal faults (Fig. 2; Hsiao et al. 1998). These normal faults extended toward southwest, probably connecting to the fault structures at northern Taiwan (Hsiao et al. 1998). Among these normal faults, the westernmost normal fault is likely to be connected to the deformation front of the current fold-thrust belt in northern Taiwan (Yu 2004). These faults were formed as a result of collapse of earliest Taiwan orogenic wedge and reactivation of thrust structures of the earliest Taiwan orogenic wedge (Hsiao et al. 1998). These normal faults are probably currently active, and the landward extension was considered active in Quaternary (Chu 1993; Hung 2013).

The NW-SE lineaments are recognized by magnetic and bathymetric data northern offshore Taiwan (Hsu et al. 1996; Liu et al. 1998; Song et al. 2000). It is also suggested that these fault structures are likely connected to the axis of the Keelung Sea Valley, Mianhua Canyon, and North Mianhua Canyon (Hsu et al. 1996). On the other hand, several bathymetrical lineaments are identified oriented with NW-SE trending in nearshore northern Taiwan (black dash lines in Fig. 2; Song et al. 2000). The individual offsets of these lineaments are estimated limited, generally less than 3 km. These lineaments are suggested to have right-lateral sense, probably reflecting the local relaxation of releasing structures after the compressive shearing under the orogeny of the convergence between the Philippine Sea Plate and Eurasian Plate since probably 2 Ma (Song et al. 2000). These nearshore lineaments are probably associated with the formation of the Keelung Sea Valley (Liu et al. 1998; Song et al. 2000). The presence of these offshore and nearshore NW-SE lineaments may reflect additional information about local controls.

2.4 Regional Magmatism

The Northern Taiwan Volcanic Zone (NTVZ) is composed of several major onland volcanic groups and offshore islands, i.e., the Pengjia Islet, Mianhu Islet, and Huaping Islet (Wang et al. 1999). Additionally, the identified submarine volcanic features are currently increasing (Hsiao et al. 1998; Tsai et al. 2017; Chang et al. 2021). It began to form at 2.8 Ma, and was previously considered as the westernmost branch of the Ryukyu volcanic arc for it is calc-alkalie andesite similar to those observed in convergent setting (Chen 1990). Succeeding petrological studies found out a spatial geochemical variation in the NTVZ, showing various degrees of melting within an ascending region of the asthenospheric mantle and similar mantle source (Chen et al. 1999; Wang et al. 1999, 2002, 2004; Chung et al. 2000; Shellnutt et al. 2014). Latest magnetic surveys showing an area of strong magnetic anomalies underlying Pengjia Islet, Menhua Islet, and Huaping Islet, indicates a possible origin of these volcanic islets (SinoTech Engineering Consultants, LTD 2016). The NTVZ is plausible to be the result of the Quaternary extensional collapse of the earliest Taiwan orogenic wedge (Wang et al. 2004; Wang and Chung 2015).

The ages of the NTVZ have been dated, mainly distributing from 2.8 to 0.2 Ma. Three subgroups of before 2.6 Ma, 2 ~ 1 Ma, and after 1 Ma can be further identified (Figs. 1 and 2, Wang et al. 2004). The first age group, including the Tatun Volcanic Group (2.8 Ma), Mianhua Islet (2.6 Ma), and Sekibisho (2.6 Ma) may represent the earliest signals of the post-collision (Fig. 2). The second age group is mainly composed of the volcanic edifice formed at the Pengjia Islet (2.1 Ma), the Tatun Volcanic Group (1.5 Ma), and Keelung Volcanic Group (1.4 Ma) (Fig. 2). The age of second group may be similar to the onset of the deposition upon the regional unconformity that represents the onset of fault-controlled subsidence (Chang et al. 2017). The third age group is mainly not younger than 0.2 Ma (Tsaolingshan: 0.3 Ma; Kobisho: 0.2 Ma), probably suggesting that 0.2 Ma may represent the age when volcanic events had ceased (Fig. 2).

In the NTVZ, the Tatun Volcanic Group is located in Taipei, the administrated city of Taiwan, and is also only few kilometers from two nuclear power plants. Soil-gas surveys reveal that Helium and CO2 here include mantle contribution, suggesting the existence of magmatic activities (Yang et al. 1999; Ohba et al. 2010; Wen et al. 2016). The volcano-hydrothermal systems are also active at Tatun Volcano Group (Konstantinou et al. 2007; Rontogianni et al. 2012). Recently, a deep, 350 km^3-sized magma reservoirs beneath the Taipei metropolis has been geophysically determined by S-wave shadows and P-wave delays (Lin 2016). This existing magma chamber is likely to be an active feature, representing the activities of post-collisional volcanism and associated structures.

3. METHOD

We used the multichannel seismic (MCS) data collected in 2014 by Taiwanese research vessel Ocean Researcher II. The source energy was shoot via a 210-cubic inch generator-injector (GI) gun with shot interval of 37.5 m. The reflection seismic data were acquired through a 24-channel, 150-meter long streamer, with a 1-ms sampling rate. The MCS data were processed by the ProMAX and KINGDOM software at the Institute of Oceanography, National Taiwan University. The data processing procedures include trace editing, geometry set up, band-pass filtering, amplitude compensation, predictive deconvolution, velocity analysis, normal move-out correction, stacking, water velocity F-K time migration, and water column mute. Bathymetric dataset is a 500-m gridded data, produced by compiling shipboard and

global dataset (Liu et al. 1998). The bathymetric charts are prepared by the GMT (Wessel et al. 2013).

Four high resolution MCS profiles covering the collapsed Late Miocene-Pleistocene wedge-top zone northern offshore Taiwan are selected (Fig. 2). Two of the profiles are oriented N-S (T1) and NW-SE (T2), which are perpendicular to structural strike of the Late Miocene-Pleistocene wedge-top zone and show the transversal structural features of the wedge-top zone. The other two profiles run NE-SW (A1 and A2), showing the volcanic edifices and normal fault structures of the Late Miocene-Pleistocene wedge-top zone. These data are intended to contribute to the understanding of the formation of post-collisional volcanisms and their possible relationship with pre-existing structures.

Our seismic interpretations are mainly based on regional stratigraphic loop-tie. The selected stratigraphic boundaries are based on several valuable previous studies (Chen and Watkins 1994; Hsiao et al. 1998; Kong et al. 2000) that reported the seismic profiles along with the depths of the age boundaries. For example, the unfilled triangle in the Fig. 2 indicates the drilling sites YCL-1 (Chen and Watkins 1994; Kong et al. 2000); and the chronostratigraphic information of the pink boundary shown on the section T1 (Fig. 4) is based on the Profile DD' in the Fig. 4 and on the age data in the Fig. 6 of the Hsiao et al. (1998). These integrated results provide regional age controls from Middle Miocene to Pleistocene, a valuable information for the development and collapse of the Taiwan orogenic wedge.

4. RESULTS

4.1 MCS Profiles Transverse to the Fold-Thrust Belt (T1 and T2)

The MCS profile T1 lies on the continental shelf area where the water depth is less than 200 m overall section. According to upwards concave and convex shape of the reflectors, a synform and two antiform structures are recognized in the MCS profile T1 (Fig. 4, SP 11500 - 13000 and SP 17000 - 19000). The Anticline A (the southern, right hand side one in the Fig. 4) has a definite narrow, near-vertical hinge zone and equally inclined fold limbs, showing a symmetrical shape. The Anticline B (the northern, left hand side one in the Fig. 4) has a relatively broader hinge zone. However, the inclination of the southern fold limb of the Anticline B is not as large as that of the northern fold limb, showing an asymmetrical form. Near seafloor, the reflectors near the hinges of those anticlines are widely truncated against seafloor.

Both Anticline A and B in profile T1 are deformed by thrusts and normal faults. At the northern sides of the anticlines they were dissected by thrusts. Among these thrusts, blind thrusts are observed located at the cratonward side of the anticlines (Fig. 4, SP 10500 - 12000; SP 16000 - 17000). At the southern sides of the anticlines, they were dissected by antithetic-sense normal faults that cut upwards upon seafloor (Fig. 4, SP 12500 - 13500; SP 18000 - 19000). These normal faults show some reverse-sense at depth. A re-activation that began with reverse fault and then succeeded by normal faults is likely to occur, indicating the change of the regional stress from convergence to extension. The northern fold limb of the Anticline A and the southern fold limb of the Anticline B constitute a synform structure convex downward (Fig. 4, SP 13000 - 17000). At shallow level of this synform structure, the reflectors are generally truncated.

Most of the MCS survey line T2 lies on the continental shelf area (Figs. 2 and 5, SP 11000 - 22000) and only SE part of the profile T2 lies below shelf break near the head of the Mianhua Canyon. In shelf area, the reflectors show a general trend of westward dipping (Fig. 5). Furthermore, the reflectors beneath seafloor are mostly truncated against seafloor, similar to those shown in the profile T1. This similarity of reflector feature between profile T1 and T2 suggest that there might be an eroded fold structure in the shelf area in the profile T2 as well. A large extent of northwestward dipping of reflectors and the absence of southeastern dipping reflectors suggest only west-limb of a fold, probably indicating a monocline structure.

The monocline structure in the profile T2 is deformed by thrusts and normal faults as those anticlines in profile T1. At northwest part of the profile T1 (Fig. 5, SP 17000 - 20000), blind thrusts at the cratonward side and nearby normal faults are recognized. Southeastward (Fig. 5, SP 12000 - 15500), the reflectors are dissected by synthetic and antithetic normal faults. The blind thrusts may be formed along with the inception of the collisional event, and the normal faulting are likely to indicate the collapse of the orogenic wedge.

4.2 MCS Profiles Parallel to the Strike of the Fold-Thrust Belt (A1 and A2)

Both MCS survey lines A1 and A2 lie on the continental shelf area, running NE-SW approximately along the western boundary of the STSFZ (Fig. 2). Drilling results provide regional chronostratigraphic framework for seismic stratigraphy (Black triangle in Fig. 6). In the eastern part of the profile A1 (Fig. 6, SP 29000 - 36000), the bathymetry does not change manifestly and seismic features are dominated by southwestward, gently dipping reflectors. However, both bathymetry and seismic features become different in western part of the profile A1 (Fig. 6, SP 23000 - 29000). With regard to the bathymetry of the western part of the profile A1, there are two seafloor pinnacles (Fig. 6, SP 22900 and SP 26400) and two local depressions (Fig. 6, SP 22500 - 23500 and SP 27000 - 28000). In western part of the profile A1, the southwestward dipping of the reflector become more inclined than those in the eastern part of the profile.

A more significant seismic feature in the western part of the profile A1 is the areas of low frequency poor

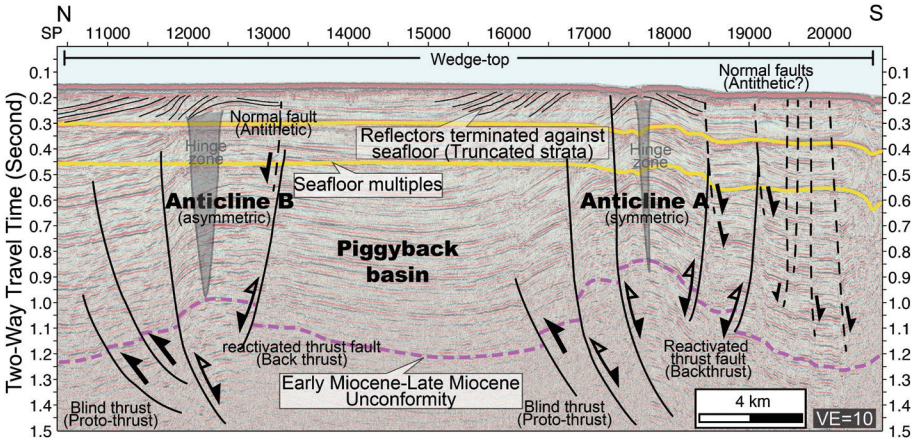

Fig. 4. Interpreted MCS profile T1. This profile runs N-S, showing fold structures along with blind thrusts and backthrusts. Near seafloor, the reflectors near the hinges of those anticlines are widely truncated against seafloor. The vertical exaggeration (VE) is 10. See Fig. 2 for location.

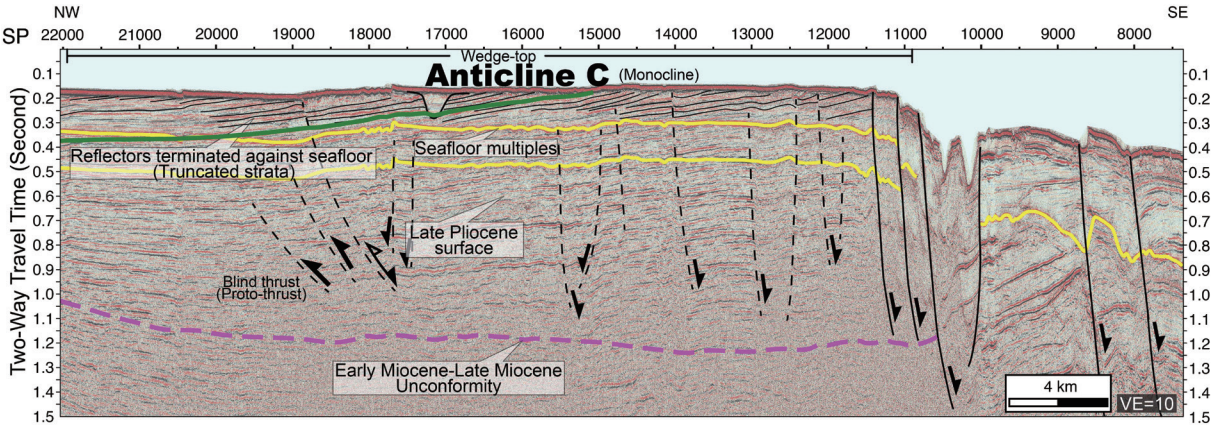

Fig. 5. Interpreted MCS profile T2. This profile runs NW-SE, showing an anticline (monocline) structure with blind thrusts. Near seafloor, the reflectors near the hinges of those anticlines are widely truncated against seafloor. The vertical exaggeration (VE) is 10. See Fig. 2 for location.

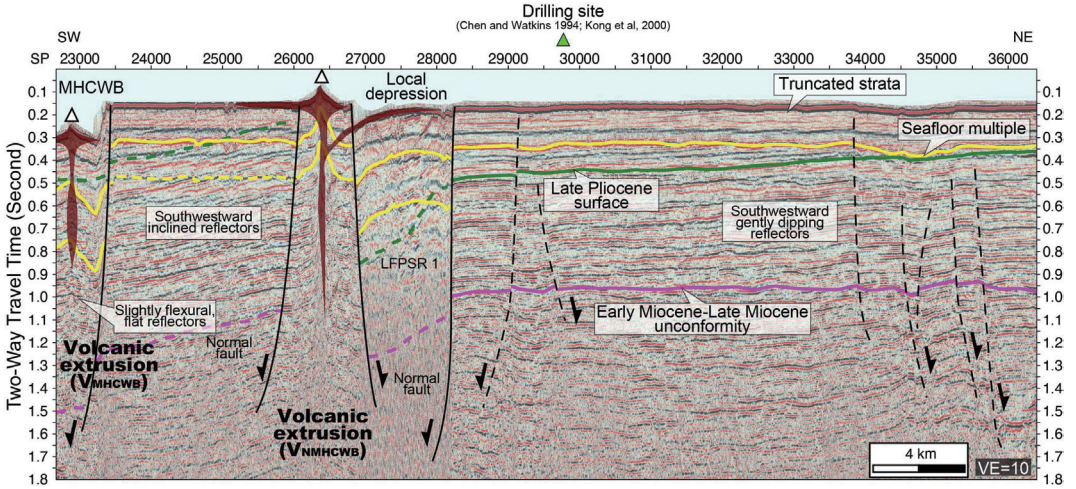

Fig. 6. Interpreted MCS profile A1. This profile runs NE-SW, showing the coexistence of volcanic influences and normal faults. The morphological feature Mianhua Sea Valley (MHCWB) is also shown at the western part of the profile. LFPSR: low frequency poor stratified reflectors. The vertical exaggeration (VE) is 10. See Fig. 2 for location.

stratified reflectors (LFPRS 1 in Fig. 6). The seafloor multiple signals here are quite strong relative to stratigraphic signals. On the other hand, these poor stratified reflectors occur just northeast from the seafloor pinnacle and are low frequency poor stratified reflectors. We consider the seismic image is generally poor under volcanic sill (Magee et al. 2016) and strong seafloor multiple may indicate a hard and solid seafloor material, probably crystallization rocks. In addition, low frequency reflectors may indicate a more homogeneous component rather than sediments. The coexistence of the bathymetric and seismic features at upper reach of MHCWB may be indicators for the volcanic extrusion (hereafter V_{NMHCWB}), and low frequency poor stratified reflectors may indicate sills lying upon/near seafloor. In addition to volcanic events, the western part of the profile A1 is also structurally dominated by normal faults. It seems that not only volcanic events but also local depressions in the western part of the profile A1 are bounded by normal faults (Fig. 6). It is thus possible that the formations of the volcanic material and normal faults are two mechanically associated events.

The MCS survey line A2 spans approximately across the Huaping Islet and Pengjia islets (Figs. 2 and 7). In the northeast part of the profile A2, the projected location of the Pengjia Islet features a seafloor pinnacle (pink filled triangle) with poor-stratified reflectors beneath (LFPSR 2 and PSR 1 in Fig. 7). It can be considered as the southeast extension of the Pengjia Islet volcanism (Hereafter V_P). Northeast of this pinnacle, we note that overlying the LFPSR 2, there is a fold structure at shallow level and is truncated by seafloor (SP 22500). Based on the volcanic sill model in Fig. 3, we interpret that there is a volcanic sill occurred between truncated fold and low frequency poor stratified reflectors, probably came from the Pengjia Islet volcanism. Once the volcanic sill started to intrude into strata, the strata were forced to uplift, forming local folds that suffered from subsequent seafloor erosion.

In the western part of the profile A2, the MHCWB (SP 30500 - 32000 in Fig. 7) occurs southwest of the projected location of the Huaping Islet (yellow filled triangle, SP 30500 - 31000 in Fig. 7). Our seismic profile shows that the MHCWB is plausible to be bounded by seafloor-cutting normal faults. In addition, the seismic characteristics beneath the MHCWB is also dominated by low frequency poor stratified reflectors (LFPSR 3 in Fig. 7), indicating a volcanic influence from seafloor/shallow level sill as can be seen in Fig. 6. Interestingly, the distribution of the LFPSR 3 seems limited by the bounding fault of the MHCWB and do not extend out of the MHCWB, suggesting that the LFPSR and the bounding fault of the MHCWB are very likely to be associated. Once the LFPSR, normal faults bounding the MHCWB and the Huaping Islet volcanism collectively occurred at very shallow level, we interpret that they may be formed very recently and probably dependently. Westwards, there is a curved strong reflector sitting very close to seafloor (SP 34000 - 35000 in Fig. 7). This reflector ascends toward northeast and has multiples underneath. Based on volcanic sill model in Fig. 3, we interpret this reflector as a combination of upward concave reflectors that represent the result of intrusive steps of volcanic sills.

5. DISCUSSION

5.1 Late Miocene-Pleistocene Wedge-Top Zone and Associated Structures

The STSFZ represents the early collisional fold-thrust belt of the Taiwan orogenic wedge (Hsiao et al. 1998). In the STSFZ, the fault blocks bounded by southeastward dipping normal faults are considered as thrust sheets formed in the early collisional event (Hsiao et al. 1998). After collision had migrated southwards and collisional stress was transferred, the thrust sheets began to slip downwards along the thrust faults, forming a series of fault blocks northern offshore Taiwan.

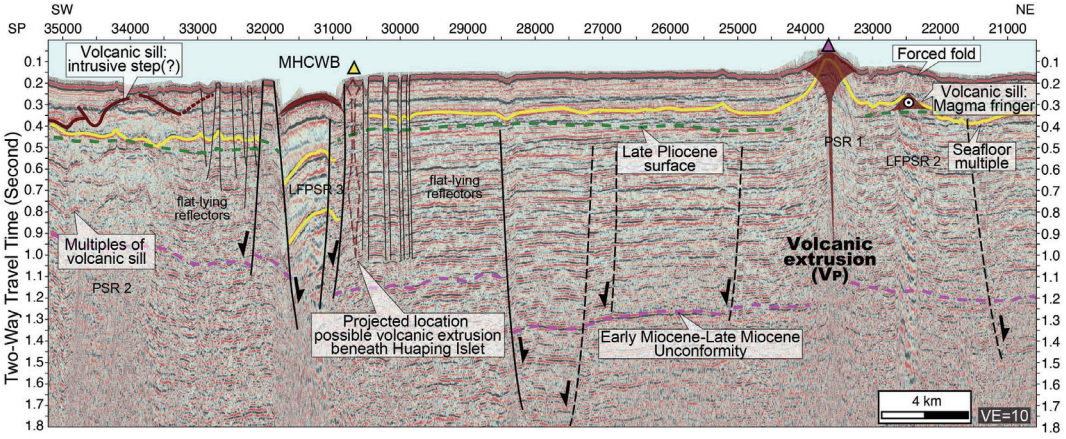

Fig. 7. Interpreted MCS profile A2. This profile runs NE-SW, showing the coexistence of possible volcanic influences, normal faults and the MHCWB. PSR: poor stratified reflectors. LFPSR: low frequency poor stratified reflectors. The vertical exaggeration (VE) is 10. See Fig. 2 for location.

The western boundary of the STSFZ represents the deformation front of the early Taiwan orogenic wedge. In the MCS profile T1, the blind thrusts at the western limbs of the Anticlines A, B, and C represent the proto-thrusts at the early stage of the Taiwan orogeny; the antithetic normal faults at the eastern limbs of the Anticlines A and B represent the back thrusts formed at the early stage of the Taiwan orogeny (Fig. 4). In addition, the synform structure between the Anticlines A and B may indicate the piggyback basin developed at the early stage of the Taiwan orogeny (Fig. 4). In the MCS profile T2, the Anticline C, which has general westward dipping reflectors, was a frontal monocline at the early stage of the Taiwan orogeny (Fig. 4). Collectively, proto-thrusts, frontal folds, back thrusts, and the piggyback basin near the western boundary of the STSFZ could be assembled, constituting a Late Miocene-Pleistocene wedge top zone at the frontal part of the early stage of the Taiwanese orogeny. The present western frontal normal fault of the STSFZ, proto-thrusts, and antithetic normal faults together, represent a collapsed wedge-top zone at a region of post-collisional extension.

Here we note that an orogenic wedge should consist of fold-thrust belt at frontal side and core complex (metamorphic basement) at rear side (Fig. 1c). The distribution of our profiles, however, cover only the frontal part of the Taiwan orogenic wedge (i.e., wedge-top) (Fig. 2) and may be irrelevant to core complex part. In addition, a wedge-top generally includes a piggyback basin by definition (DeCelles and Giles 1996) and is more applicable to our study area. The wedge-top will be better descriptive term for our study area rather than orogenic wedge.

The collapsed wedge-top of early Taiwan orogenic belt recognized by the reflectors terminated against seafloor and eroded anticlines in our MCS data provide an evolutional implication for the formation of regional landscape. Located about 200 km northeast of north Taiwan, Diaoyutai Islets (also known as Senkaku Islands) lies at the southwest end of Ryukyu Islands, mainly composed of Lower Miocene shallow marine conglomerate, sandstones and thin coal beds, and Pliocene-Pleistocene coral reef (Kizaki 1985, 1986). These islets are lying near the axis of regional fold structures (Hsiao et al. 1998). They began to be uplifted since Middle Miocene, and were subsequently influenced by Late Miocene granitoids. At least two events of intrusive diorite were recognized (Kizaki 1985, 1986; Kawano 2010). These intrusive events are previously considered as initial volcanism associated with the formation of the Okinawa Trough (Miyazaki et al. 2016).

Based on the observed reflectors terminated against seafloor and eroded anticlines in our MCS data, along with the concept of collapsed wedge-top of early Taiwan orogenic belt, we interpret that the fold underlying these islets are collapsed structures of the earliest Taiwan orogenic belt and these islands are surface part of submerged Taiwan orogenic belt. These islets may have experienced the earliest Taiwan orogeny at Middle Miocene. After the orogeny moved southwards at Late Miocene, the stress environment transferred from convergent to extension, triggering the earliest geochemical signal of the post-collision and leading to intrusive events during Late Miocene-Pliocene.

5.2 Distribution of Volcanic Associated Structures

In addition to the collapsed Late Miocene wedge-top zone structures, the northern Taiwan is largely dominated by Northern Taiwan Volcanic Zone that comprise of several volcanic groups. North of Taipei Basin, Tatun Volcanic Group covers large area of northern Taiwan; offshore, Pehngjia Islet, Huaping Islet, and Mianhua Islet resulted from andesitic and basaltic magma (Chen 1990). Based on geophysical surveys, more submerged volcanic associated features are observed offshore northern Taiwan (Hsiao et al. 1998; Chang et al. 2017). In this study, a volcanic extrusion V_{NMHCWB} is observed at the eastern side of the MHCWB in the profile T1 (Fig. 6, SP 26000 - 27000). Southeast of the Pengjia Islet, another volcanic extrusion V_P is identified by seafloor pinnacle and low frequency reflectors, showing the extension of the Pengjia Islet volcanism (Fig. 7, SP 22000 - 24000). In addition, the projected location of the Huaping Islet is westerly bounded by the eastern wall of the MHCWB and is likely to be formed by normal fault structures (Fig. 7, SP 30500 - 32000). These volcanic extrusions observed in our MCS data are generally close to faults structures.

According to distribution of the offshore volcanic extrusions, it seems that most of them are located along the western boundary of the STSFZ, including the Huaping Islet and Mianhua Islet (Fig. 2; Hsiao et al. 1998). This consistence of the distribution between fault structures and volcanic extrusion probably indicates that the formation of these volcanic extrusions may greatly benefited by the existence of the NE-SW faults. However, we note that the area of the V_H is greater than the other offshore volcanic extrusions, and that the V_H is located at the intersection between the western boundary fault of the STSFZ and the course of the MHCWB (Fig. 2). It is thus possible that although the western boundary fault of the STSFZ provide the dominating regional control, there was an additional control that effectively contributed to the volume of the V_H.

Except for those volcanic extrusions located along the NE-SW boundary fault of the STSFZ, the V_{NMHCWB} observed in this study is located about 20 km away from the Western boundary of the STSFZ (Fig. 2). Since the V_{NMHCWB} is possibly bounded by normal fault to both southwest and northeast side (Fig. 6), we propose that the formation of the V_{NMHCWB} is likely to be benefited by fault structures. However, the V_{NMHCWB} is located north of the NE-SW fault zone of the STSFZ. It seems that the governing fault structures that led to the formation of the V_{NMHCWB} are more likely to be local

fault structures, rather than the NE-SW faults of the south.

To sum up, the NE-SW faults in northern offshore Taiwan are likely dominating and may provide major conduits for post-collisional magma ascending, leading to a number of volcanic extrusions in northern offshore Taiwan. On the other hand, a secondary control on the formation of the of volcanic extrusion is very likely to be provided by a group of the NW-SE faults. They could be evidenced by observed offshore volcanic extrusion along the NW-SE trend and the existence of the relatively larger volume of the V_H volcanism.

5.3 Summary: Structural Implication for Regional Volcanisms

In early 1990s, the volcanisms in northern Taiwan had been considered as the southwesternmost part of the Ryukyu Arc (Chen 1990). Subsequently, Hsiao et al. (1998) demonstrated the Late Miocene-Pleistocene structural evolution of the STSFZ in response to post-collisional mountain collapse northern offshore Taiwan, based on excellent structural analyses MCS dataset. New petrological and geochemical results provide more information on magma provenance of Quaternary volcanisms in the NTVZ (Wang et al. 2004): both structural framework evolution and volcanisms reflect a post-collision process. The interplay between magma activities and fault structures northern offshore Taiwan should be certain. While as revealed by bathymetric viewpoint (Song et al. 2000), it seems some detailed features like NW-SE faults are under-observation. More observations to better reveal the evolutionary contexts are required.

In this study, Figs. 4 and 5 have shown a series of protothrusts, anticlines and back thrusts along with the piggyback basin bounded by anticlines, indicating the Late Miocene wedge-top zone upon the fold-thrust belt. Once the Pleistocene post-collisional extension started to occur, these Late Miocene convergent structures are highly likely to serve as weak zones for extensional deformation, allowing Pleistocene normal faulting to slip along. The Figs. 6 and 7 have shown several volcanic islets and extrusions formed nearby dominating NE-SW normal fault (the western boundary of the STSFZ) and sea valley that bounded by probably secondary normal faults, indicating the influence of post-collisional extension. It is thus possible that NE-SW structures significantly contributed to post-collision volcanism at first place, and secondary normal fault structures probably in NW-SE trends provide local control on volcanisms.

On the basis of the unconformities recently recognized northern offshore Taiwan in new MCS data (Chang et al. 2017) and volcanic features observed in this study, an updated interpretation of evolutionary history northern offshore Taiwan that integrate the structural framework and volcanisms is presented as follows. The earliest Taiwan orogeny occurred in Late Miocene, forming fold-thrust belt with a series of compressional structures northern offshore Taiwan (Fig. 8a). After reaching the culmination of orogenic activities (~2.6 Ma; Fig. 8b), the stress field of northern Taiwan has changed from collision to extension and the mountain range in northern offshore Taiwan began to collapse, forming the NE-SW faults. In the meantime, extensional post-collisional magmatism that contributed by significant upwelling of asthenosphere was also about to occur (Wang et al. 2004), probably marked by the beginning of the NTVZ. Along the extensional NE-SW faults, the magma started to ascend and volcanic extrusions were formed accordingly.

Subsequently, the re-opening of the Okinawa Trough at ~2 Ma may indicate that the collision-thickened lithosphere had been removed, probably along with the flipping of plate convergence polarity and the propagation of the Philippine Sea Plate (Fig. 8c; Teng 1996; Wang et al. 2004). We note that away from NE-SW faults, the Pengjia Islet was formed during this stage, suggesting that the Pengjia Islet volcanism may be significantly contributed by local controls. This local control may strengthen the volcanisms near Huaping Islet as well, increasing the volume of the Huaping Islet volcanism.

The second stage of the NTVZ occurred around 1.5 Ma (Fig. 8d). It seems to be the time that the extensional basin in northern offshore Taiwan started to receive post-collisional sediments. It was also the time that northern offshore Taiwan was governed by fault-controlled subsidence and the rotation of the fault blocks, reflecting a mechanical stretching at early stages of extensional basin development (Chang et al. 2017). Afterwards, the third stage of the NTVZ occurred during 1 ~ 0.2 Ma (Fig. 8e). It was the period that Taipei Basin started to form and received the earliest deposits (0.4 Ma; Teng et al. 2001). The diachronous development of north offshore Taiwan in the north and Taipei Basin in the south reflect the sequential collapse of the northernmost Taiwan orogenic wedge. This fault-controlled subsidence may last until late Quaternary (~0.2 Ma; Fig. 8f).

5.4 Implication for Future Geohazards

It appears that there is a close relationship between fault structures and volcanisms northern offshore Taiwan. Since these faults northern offshore Taiwan mainly resulted from the Late Pliocene mountain collapse, southwest continuation of mountain collapse may play an important role in future volcanisms. On the other hand, although the main NE-SW faults may provide a regional control and may ascribe for most of volcanisms northern offshore Taiwan, we note that there should be some local controls that had effectively contributed. Collectively, we suggested that the extension of NE-SW fault should receive more concerns, and the combination of these structural controls may lead to higher potential sites for future geohazards.

6. CONCLUSION

Based on multichannel seismic data northern offshore Taiwan, we revisited the post-collisional and volcanic features in the Late Miocene-Pleistocene wedge-top of the early Taiwan orogenic wedge. Seismic data transverse to wedge-top zone show the asymmetric and symmetric folds, along with blind thrusts and back thrusts. Seismic data parallel to the axis of the wedge-top zone show the volcanic features of poor stratified reflectors, forced fold and intrusive step along and away from dominating normal fault structures. Since the volcanic extrusions and normal faults are probably associated events, we suggest that the formation of post-collisional extensional volcanism northern offshore Taiwan was probably formed relevant to inherited primary and secondary fault structures. The wedge-top zone was formed at frontal part of the early Taiwan orogenic wedge in Late Miocene. Subsequent change of regional stress from convergence to extension led to the mountain collapse as well as primary and secondary normal faults. Thus, these post-collisional

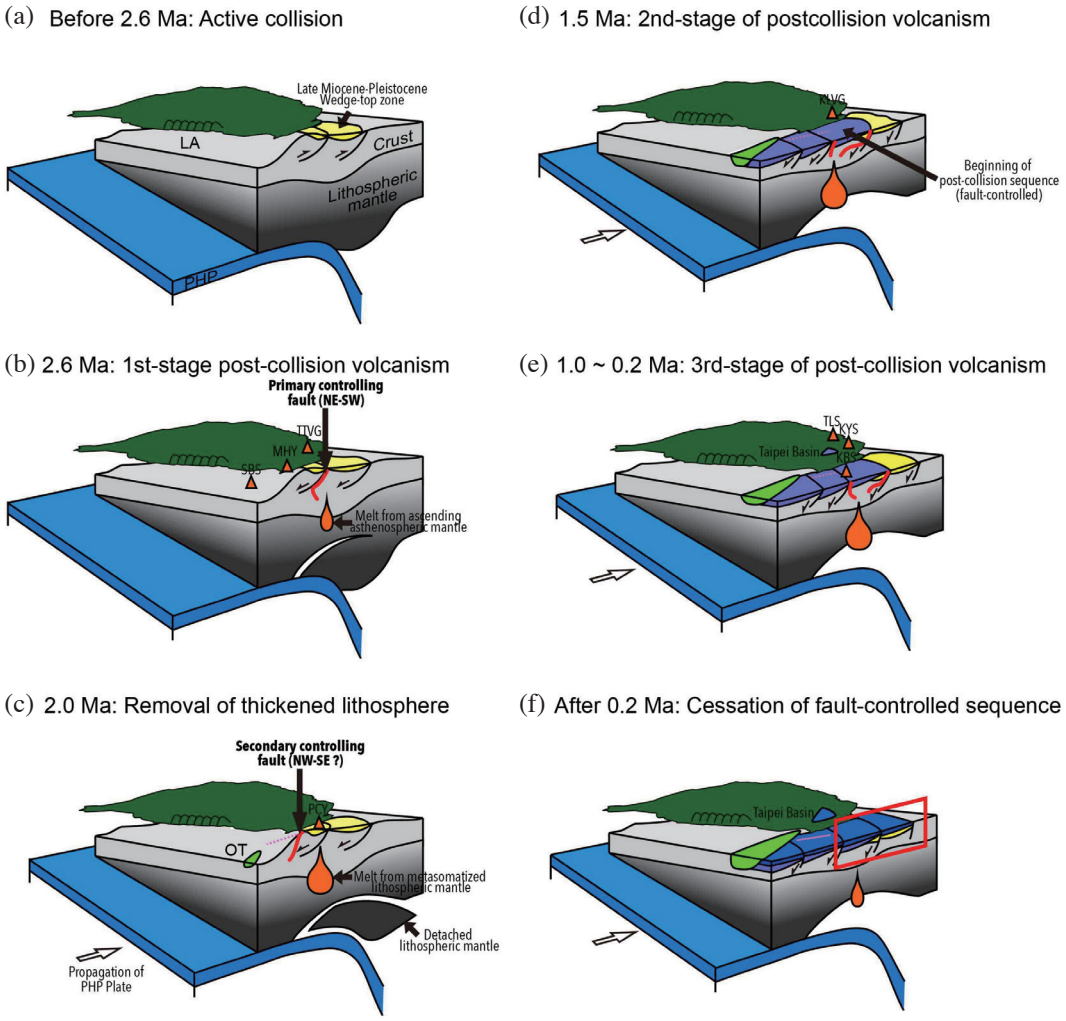

Fig. 8. Schematic cartoons for tectonic evolution northern offshore Taiwan. (a) The northernmost Taiwan orogeny in Late Miocene-Pleistocene, forming fold-thrust belt with a series of compressional structures northern offshore Taiwan. (b) After reaching the culmination of orogenic activities, the stress field of northern Taiwan has changed from collision to extension and the mountain range in northern offshore Taiwan began to collapse. Along the extensional faults, the magma started to ascend and volcanic extrusions were formed accordingly. (c) The re-opening of the Okinawa Trough at ~2 Ma may indicate that the collision-thickened lithosphere had been removed. We note that the formation of the Pengjia Islet was during this stage and was away from post-collision fault, suggesting that the Pengjia Islet volcanism may be effectively contributed by local controls, probably associated with releasing strike-slip structures. (d) The second stage of the NTVZ occurred around 1.5 Ma. It seems the time that the extensional basin in northern offshore Taiwan started to receive post-collisional sediments. It was also the time that northern offshore Taiwan was governed by fault-controlled subsidence and the rotation of the fault blocks, reflecting a mechanical stretching at early stages of extensional basin development. (e) The third stage of the NTVZ. It was the period that Taipei Basin started to form and received the earliest deposits. The diachronous development of north offshore Taiwan in the north and Taipei Basin in the south reflect the sequential collapse of the northernmost Taiwan orogenic wedge. (f) This fault-controlled subsidence may last until late Quaternary.

normal faults are mechanically weak, probably capable of providing pathways for the Pleistocene-present volcanisms northern offshore Taiwan to occur along. The facilitation of post-collisional fault structures as transportation routes for deep material to migrate along may be important for the formation of the Quaternary volcanism extrusions northern offshore Taiwan.

Acknowledgements We acknowledge the technical assistance from Ms. Yu-Fang Ma and Mr. Hsin-Sung Hsieh of Marine Exploration Instrumental Center, National Taiwan University. We thank captain and crew members of R/V Ocean Researcher II for help with data collection. We also thank Mr. Yuan-Wei Lee and Mr. Jian-Ming Chen of Offshore Exploration & Production Division, Exploration & Production Business Division, Chinese Petroleum Company, Taiwan and Prof. Jui-Lin Chang, Dr. Shyh-Chin Lan, and Mr. Yen-Chun Lin of GeoResource Research Center, National Cheng Kung University for their encouragement. We thank Bureau of Mine, Ministry of Economic Affair of Taiwan, for the financial support. JH was supported by Postdoctoral Research Abroad Program (106-2917-I-564-050) from Ministry of Science and Technology of Taiwan during the period of manuscript preparation.

REFERENCE

Chang, J.-H., H.-S. Yu, H.-H. Hsu, and C.-S. Liu, 2012: Forebulge migration in late Cenozoic Western Taiwan Foreland Basin. *Tectonophysics*, **578**, 117-125, doi: 10.1016/j.tecto.2011.09.007. [Link]

Chang, J.-H., E. Y.-C. Yang, H.-H. Hsu, C.-C. Su, C.-S. Liu, S.-D. Chiu, Y.-F. Ma, Y.-W. Li, Y.-C. Lin, and J.-S. Shen, 2017: Seismic stratigraphic features of the Late Miocene-present unconformities and related seismic units, northern offshore Taiwan. In: Aiello, G. (Ed.), Seismic and Sequence Stratigraphy and Integrated Stratigraphy - New Insights and Contributions, InTechOpen, London, United Kingdom, doi: 10.5772/intechopen.70819. [Link]

Chang, J.-H., E. Y.-C. Yang, H.-H. Hsu, T.-T. Chen, C.-S. Liu, and S.-D. Chiu, 2021: Igneous Activity and Structural Development of the Mianhua Terrace, Offshore North Taiwan. *Minerals*, **11**, 303, doi: 10.3390/min11030303. [Link]

Chen, C. H., 1990: Igneous Rocks of Taiwan, Central Geological Survey Special Publication, Vol. 1, 137 pp. (in Chinese)

Chen, C. H., C.-H. Chen, S. A. Mertzman, and J. J. S. Shen, 1999: An unusual late Cenozoic volcanic zone in northern Taiwan Behind the southern Okinawa Trough. *J. Geol. Soc. China*, **42**, 593-612.

Chen, T.-T. and J. S. Watkins, 1994: Structure and stratigraphy of South Pengchiahsu Basin, northern offshore Taiwan. *Petrol. Geol. Taiwan*, **29**, 127-170.

Chiang, C.-S., H.-S. Yu, and Y.-W. Chou, 2004: Characteristics of the wedge-top depozone of the southern Taiwan foreland basin system. *Basin Res.*, **16**, 65-78, doi: 10.1111/j.1365-2117.2004.00222.x. [Link]

Chu, C.-J., 1993: Paleostress analysis of the Hsinchuang-Chinshin Fault. Master Thesis, National Taiwan University, Taipei City, Taiwan, 81 pp.

Chung, S.-L., S.-L. Wang, R. Shinjo, C.-S. Lee, and C.-H. Chen, 2000: Initiation of arc magmatism in an embryonic continental rifting zone of the southernmost part of Okinawa Trough. *Terr. Nova*, **12**, 225-230, doi: 10.1046/j.1365-3121.2000.00298.x. [Link]

Chung, S.-L., K.-L. Wang, A. J. Crawford, V. S. Kamenetsky, C.-H. Chen, C.-Y. Lan, and C.-H. Chen, 2001: High-Mg potassic rocks from Taiwan: Implications for the genesis of orogenic potassic lavas. *Lithos*, **59**, 153-170, doi: 10.1016/s0024-4937(01)00067-6. [Link]

Chung, S.-L., M.-F. Chu, Y. Zhang, Y. Xie, C.-H. Lo, T.-Y. Lee, C.-Y. Lan, X. Li, Q. Zhang, and Y. Wang, 2005: Tibetan tectonic evolution inferred from spatial and temporal variations in post-collisional magmatism. *Earth-Sci. Rev.*, **68**, 173-196, doi: 10.1016/j.earscirev.2004.05.001. [Link]

DeCelles, P. G., 2011: Foreland basin systems revisited: Variations in response to tectonic settings. In: Busby, C. and A. Azor (Eds.), Tectonics of Sedimentary Basins: Recent Advances, Blackwell Publishing Ltd., 405-426, doi: 10.1002/9781444347166.ch20. [Link]

DeCelles, P. G. and K. A. Giles, 1996: Foreland basin systems. *Basin Res.*, **8**, 105-123, doi: 10.1046/j.1365-2117.1996.01491.x. [Link]

Hsiao, C.-L., H.-H. Ting, T.-Y. Chiou, and W.-W. Mei, 1994: The tectonic evolution of Taiwan-Sinzi Zone offshore northern Taiwan and hydrocarbon potential. *Exploration and Development Research Report*, **17**, 67-81.

Hsiao, L.-Y, K.-A. Lin, S.-T. Huang, and L. S. Teng, 1998: Structural characteristics of the southern Taiwan-Sinzi Folded Zone. *Petrol. Geol. Taiwan*, **32**, 133-153.

Hsu, S.-K., J.-C. Sibuet, S. Monti, C.-T. Shyu, and C.-S. Liu, 1996: Transition between the Okinawa Trough backarc extension and the Taiwan collision: New insights on the southernmost Ryukyu subduction zone. *Mar. Geophys. Res.*, **18**, 163-187, doi: 10.1007/bf00286076. [Link]

Huang, S.-T., H.-H. Ting, R.-C. Chen, W.-R. Chi, C.-C. Hu, and H.-C. Shen, 1992: Basinal framework and tectonic evolution of offshore northern Taiwan. *Petrol. Geol. Taiwan*, **27**, 47-72.

Hung, T.-I., 2013: Geomorphologic study offshore the Jingshan area. Master Thesis, National Taiwan University, Taipei City, Taiwan, 54 pp.

Jackson, C. A.-L., N. Schofield, and B. Golenkov, 2013:

Geometry and controls on the development of igneous sill-related forced folds: A 2-D seismic reflection case study from offshore southern Australia. *Geol. Soc. Am. Bull.*, **125**, 1874-1890, doi: 10.1130/b30833.1. [Link]

Jolivet, L. and J.-P. Brun, 2010: Cenozoic geodynamic evolution of the Aegean. *Int. J. Earth Sci.*, **99**, 109-138, doi: 10.1007/s00531-008-0366-4. [Link]

Kawano, Y., 2010: Diorite in Senkaku Islands. In: Sano, H. (Ed.), Regional Geology of Japan – Kyushu and Okinawa, Asakura Publishing.

Kizaki, K., 1985: Geology of Ryukyu Arc, Okinawa Times, Naha, Japan, 278 pp.

Kizaki, K., 1986: Geology and tectonics of the Ryukyu Islands. *Tectonophysics*, **125**, 193-207, doi: 10.1016/0040-1951(86)90014-4. [Link]

Kong, F., L. A. Lawver, and T.-Y. Lee, 2000: Evolution of the southern Taiwan–Sinzi Folded Zone and opening of the southern Okinawa trough. *J. Asian Earth Sci.*, **18**, 325-341, doi: 10.1016/s1367-9120(99)00062-0. [Link]

Konstantinou, K. I., C.-H. Lin, and W.-T. Liang, 2007: Seismicity characteristics of a potentially active quaternary volcano: The Tatun Volcano Group, northern Taiwan. *J. Volcanol. Geotherm. Res.*, **160**, 300-318, doi: 10.1016/j.jvolgeores.2006.09.009. [Link]

Lin, C.-H., 2016: Evidence for a magma reservoir beneath the Taipei metropolis of Taiwan from both S-wave shadows and P-wave delays. *Sci. Rep.*, **6**, 39500, doi: 10.1038/srep39500. [Link]

Liu, C.-S., S.-Y. Liu, S. E. Lallemand, N. Lundberg, and D. L. Reed, 1998: Digital elevation model offshore Taiwan and its tectonic implications. *Terr. Atmos. Ocean. Sci.*, **9**, 705-738, doi: 10.3319/TAO.1998.9.4.705(TAICRUST). [Link]

Liu, T.-K., S. Hsieh, Y.-G. Chen, and W.-S. Chen, 2001: Thermo-kinematic evolution of the Taiwan oblique-collision mountain belt as revealed by zircon fission track dating. *Earth Planet. Sci. Lett.*, **186**, 45-56, doi: 10.1016/s0012-821x(01)00232-1. [Link]

Magee, C., C. A.-L. Jackson, and N. Schofield, 2013: The influence of normal fault geometry on igneous sill emplacement and morphology. *Geology*, **41**, 407-410, doi: 10.1130/G33824.1. [Link]

Magee, C., J. D. Muirhead, A. Karvelas, S. P. Holford, C. A. Jackson, I. D. Bastow, N. Schofield, C. T. Stevenson, C. McLean, W. McCarthy, and O. Shtukert, 2016: Lateral magma flow in mafic sill complexes. *Geosphere*, **12**, 809-841, doi: 10.1130/GES01256.1. [Link]

Miyazaki, K., M. Ozaki, M. Saito, and S. Toshimitsu, 2016: The Kyushu–Ryukyu Arc. In: Moreno, T., S. Wallis, T. Kojima, and W. Gibbons (Eds.), The Geology of Japan, Geological Society London, doi: 10.1144/GOJ.6. [Link]

Ohba, T., T. Sawa, N. Taira, T. F. Yang, H. F. Lee, T. F. Lan, M. Ohwada, N. Morikawa, and K. Kazahaya, 2010: Magmatic fluids of Tatun volcanic group, Taiwan. *Appl. Geochem.*, **25**, 513-523, doi: 10.1016/j.apgeochem.2010.01.009. [Link]

Pace, P., V. Pasqui, E. Tavarnelli, and F. Calamita, 2017: Foreland-directed gravitational collapse along curved thrust fronts: Insights from a minor thrust-related shear zone in the Umbria–Marche belt, central-northern Italy. *Geol. Mag.*, **154**, 381-392, doi: 10.1017/S0016756816000200. [Link]

Planke, S., T. Rasmussen, S. S. Rey, and R. Myklebust, 2005: Seismic characteristics and distribution of volcanic intrusions and hydrothermal vent complexes in the Voring and More basins. In: Doré, A. G. and B. A, Vining (Eds.), Petroleum Geology: North-West Europe and Global Perspectives - Proceedings of the 6th Petroleum Geology Conference, Vol. 6, Geological Society, London, 833-844, doi: 10.1144/0060833. [Link]

Pollard, D. D., O. H. Muller, and D. R. Dockstader, 1975: The form and growth of fingered sheet intrusions. *Geol. Soc. Am. Bull.*, **86**, 351-363, doi: 10.1130/0016-7606(1975)86<351:TFAGOF>2.0.CO;2. [Link]

Reeves, J., C. Magee, and C. A.-L. Jackson, 2018: Unravelling intrusion-induced forced fold kinematics and ground deformation using 3D seismic reflection data. *Volcanica*, **1**, 1-17, doi: 10.30909/vol.01.01.0117. [Link]

Rontogianni, S., K. I. Konstantinou, and C.-H. Lin, 2012: Multi-parametric investigation of the volcano-hydrothermal system at Tatun Volcano Group, northern Taiwan. *Nat. Hazards Earth Syst. Sci.*, **12**, 2259-2270, doi: 10.5194/nhess-12-2259-2012. [Link]

Schofield, N., C. Stevenson, and T. Reston, 2010: Magma fingers and host rock fluidization in the emplacement of sills. *Geology*, **38**, 63-66, doi: 10.1130/G30142.1. [Link]

Schofield, N. J., D. J. Brown, C. Magee, and C. T. Stevenson, 2012: Sill morphology and comparison of brittle and non-brittle emplacement mechanisms. *J. Geol. Soc.*, **169**, 127-141, doi: 10.1144/0016-76492011-078. [Link]

Seghedi, I., L. Maţenco, H. Downes, P. R. D. Mason, A. Szakács, and Z. Pécskay, 2011: Tectonic significance of changes in post-subduction Pliocene–Quaternary magmatism in the south east part of the Carpathian–Pannonian Region. *Tectonophysics*, **502**, 146-157, doi: 10.1016/j.tecto.2009.12.003. [Link]

Shellnutt, J. G., A. Belousov, M. Belousova, K.-L. Wang, and G. F. Zellmer, 2014: Generation of calc-alkaline andesite of the Tatun volcanic group (Taiwan) within an extensional environment by crystal fractionation. *Int. Geol. Rev.*, **56**, 1156-1171, doi: 10.1080/00206814.2014.921865. [Link]

SinoTech Engineering Consultants, LTD, 2016: Final report of extended geological survey for operating nuclear power plants (open version).

Song, G.-S., Y.-C. Chang, and C.-P. Ma, 1997: Characteristics of submarine topography off northern Taiwan. *Terr. Atmos. Ocean. Sci.*, **8**, 461-480, doi: 10.3319/TAO.1997.8.4.461(O). [Link]

Song, G.-S., C.-P. Ma, and H.-S. Yu, 2000: Fault-controlled genesis of the Chilung Sea Valley (northern Taiwan) revealed by topographic lineaments. *Mar. Geol.*, **169**, 305-325, doi: 10.1016/s0025-3227(00)00084-0. [Link]

Spacapan, J. B., O. Galland, H. A. Leanza, and S. Planke, 2017: Igneous sill and finger emplacement mechanism in shale-dominated formations: A field study at Cuesta del Chihuido, Neuquén Basin, Argentina. *J. Geol. Soc.*, **174**, 422-433, doi: 10.1144/jgs2016-056. [Link]

Teng, L. S., 1990: Geotectonic evolution of late Cenozoic arc-continent collision in Taiwan. *Tectonophysics*, **183**, 57-76, doi: 10.1016/0040-1951(90)90188-e. [Link]

Teng, L. S., 1992: Geotectonic evolution of Tertiary continental margin basins of Taiwan. *Petrol. Geol. Taiwan*, **27**, 1-19.

Teng, L. S., 1996: Extensional collapse of the northern Taiwan mountain belt. *Geology*, **24**, 949-952, doi: 10.1130/0091-7613(1996)024<0949:ECOTNT>2.3.CO;2. [Link]

Teng, L. S., C. T. Lee, C.-H. Peng, W.-F. Chen, and C.-J. Chu, 2001: Origin and geological evolution of the Taipei Basin, northern Taiwan. *West. Pac. Earth Sci.*, **1**, 115-142.

Tsai, C.-H., S.-K. Hsu, S.-S. Lin, T. F. Yang, S.-Y. Wang, W.-B. Doo, H.-F. Lee, T. Lan, J.-C. Huang, and C.-W. Liang, 2017: The Keelung Submarine Volcano in the near-shore area of northern Taiwan and its tectonic implication. *J. Asian Earth Sci.*, **149**, 86-92, doi: 10.1016/j.jseaes.2017.01.022. [Link]

Valentine, G. A. and K. E. C. Krogh, 2006: Emplacement of shallow dikes and sills beneath a small basaltic volcanic center – The role of pre-existing structure (Paiute Ridge, southern Nevada, USA). *Earth Planet. Sci. Lett.*, **246**, 217-230, doi: 10.1016/j.epsl.2006.04.031. [Link]

Wang, K.-L. and S.-L. Chung, 2015: Igneous rock and magmatic activities. In: Chen, W.-S. (Ed.), An Introduction of Taiwan Geology, Geological Society Located in Taipei.

Wang, K.-L., S.-L. Chung, C.-H. Chen, R. Shinjo, T. F. Yang, and C.-H. Chen, 1999: Post-collisional magmatism around northern Taiwan and its relation with opening of the Okinawa Trough. *Tectonophysics*, **308**, 363-376, doi: 10.1016/s0040-1951(99)00111-0. [Link]

Wang, K.-L., S.-L. Chung, C.-H. Chen, and C.-H. Chen, 2002: Geochemical constraints on the petrogenesis of high-Mg basaltic andesites from the Northern Taiwan Volcanic Zone. *Chem. Geol.*, **182**, 513-528, doi: 10.1016/s0009-2541(01)00338-2. [Link]

Wang, K.-L., S.-L. Chung, S. Y. O'reilly, S.-S. Sun, R. Shinjo, and C.-H. Chen, 2004: Geochemical Constraints for the Genesis of Post-collisional Magmatism and the Geodynamic Evolution of the Northern Taiwan Region. *J. Petrol.*, **45**, 975-1011, doi: 10.1093/petrology/egh001. [Link]

Wen, H.-Y., T. F. Yang, T. F. Lan, H.-F. Lee, C.-H. Lin, Y. Sano, and C.-H. Chen, 2016: Soil CO_2 flux in hydrothermal areas of the Tatun Volcano Group, Northern Taiwan. *J. Volcanol. Geotherm. Res.*, **321**, 114-124, doi: 10.1016/j.jvolgeores.2016.04.021. [Link]

Wessel, P., W. H. F. Smith, R. Scharroo, J. Luis, and F. Wobbe, 2013: Generic mapping tools: Improved version released. *Eos, Trans. AGU*, **94**, 409-410, doi: 10.1002/2013EO450001. [Link]

Williams, H., S. Turner, S. Kelley, and N. Harris, 2001: Age and composition of dikes in Southern Tibet: New constraints on the timing of east-west extension and its relationship to postcollisional volcanism. *Geology*, **29**, 339-342,doi:10.1130/0091-7613(2001)029<0339:AACODI>2.0.CO;2. [Link]

Yang, T. F., Y. Sano, and S. R. Song, 1999: $^3He/^4He$ ratios of fumaroles and bubbling gases of hot springs in Tatun volcano group, North Taiwan. *IL Nuovo Cimento*, **22C**, 281-286.

Yu, H.-S., 2004: Nature and distribution of the deformation front in the Luzon Arc-Chinese continental margin collision zone at Taiwan. *Mar. Geophys. Res.*, **25**, 109-122, doi: 10.1007/s11001-005-0737-1. [Link]

Yu, H.-S. and Y.-W. Chou, 2001: Characteristics and development of the flexural forebulge and basal unconformity of Western Taiwan Foreland Basin. *Tectonophysics*, **333**, 277-291, doi: 10.1016/s0040-1951(00)00279-1. [Link]

Yu, H.-S. and J. Chow, 1997: Cenozoic basins in northern Taiwan and tectonic implications for the development of the eastern Asian continental margin. *Palaeogeogr. Palaeoclimatol. Palaeoecol.*, **131**, 133-144, doi: 10.1016/s0031-0182(96)00124-1. [Link]

Yu, H.-S. and G.-S. Song, 2000: Physiographic and Geologic Frameworks of the Shelf-Slope Region off Northeastern Taiwan. *Acta Oceanogr. Taiwan.*, **38**, 1-22.